

Multivariate t -Mixtures-Model-based Cluster Analysis of BATSE Catalog Establishes Importance of All Observed Parameters, Confirms Five Distinct Ellipsoidal Sub-populations of Gamma Ray Bursts

Souradeep Chattopadhyay,¹ and Ranjan Maitra,^{1*}

¹ *Department of Statistics, Iowa State University, 2438, Osborn Drive, Ames, Iowa 50011-1090, USA*

Accepted XXX. Received YYY; in original form ZZZ

ABSTRACT

Determining the kinds of Gamma Ray Bursts has been of interest to astronomers for many years. We analyzed 1599 GRBs from the BATSE 4Br catalogue using t -mixtures-model-based clustering on all nine observed parameters (T_{50} , T_{90} , F_1 , F_2 , F_3 , F_4 , P_{64} , P_{256} , P_{1024}) and found evidence of five homogeneous groups of Gamma Ray Bursts. Our results further refine the findings of Chattopadhyay & Maitra (2017) by providing groups that are more distinct. We also classify 374 GRBs in the BATSE catalog that have incomplete information in some of the observed variables (mainly the four time integrated fluences F_1 , F_2 , F_3 and F_4) to the five groups obtained using the 1599 GRBs having complete information in all the observed variables. We found that GRBs having incomplete parameter reads have higher peak flux density compared to the bursts with all observed parameters; thus bursts with incomplete observations are mostly high energy bursts.

Key words: methods: data analysis - Astronomical instrumentation, methods, and techniques; methods: statistical - Astronomical instrumentation, methods, and techniques; gamma-rays: general - Resolved and unresolved sources as a function of wavelength

1 INTRODUCTION

Gamma Ray Bursts (GRB) are among the brightest electromagnetic events known in space and have been actively researched ever since their discovery in the late 1960s, mainly because researchers hypothesize that these celestial events hold the clue to the understanding of numerous mysteries of the outer cosmos. The source and nature of these highly explosive events remain unresolved (Chattopadhyay et al. 2007) with researchers hypothesizing that GRBs are a heterogeneous group of several subpopulations (*e.g.*, Mazets et al. 1981; Norris et al. 1984; Dezalay et al. 1992) but there are questions on the number of these groups and their underlying properties. Most analyses pertaining to GRBs have been carried out using duration variable T_{90} (or the time by which 90% of the flux arrive) while a few analysts used hardness ratios (H_{32} and H_{321}) in addition to T_{90} . Kouveliotou et al. (1993) found that the $\log_{10} T_{90}$ variable from the Burst and Transient Source Experiment (BATSE) Catalogue follows a bimodal distribution and established the

two well-known classes of GRBs, namely the short duration ($T_{90} < 2s$) and the long duration bursts ($T_{90} > 2s$). The progenitors of short duration bursts are thought to be merger of two neutron stars (NS-NS) or a neutron star with a black hole (NS-BH) (Nakar 2007) while that of long duration bursts are largely believed to be associated with the collapse of massive stars (Paczynski 1998; Woosley & Bloom 2006). Many other authors subsequently carried out several experimental studies using BATSE and other catalogues and reported a variety of findings. Pendleton et al. (1997) used 882 GRBs from the BATSE catalog to perform spectral analysis and found two classes of bursts – the High Energy (HE) and the Non High Energy (NHE) Bursts. Horváth (1998) proposed the presence of a third class of GRBs by making two and three Gaussian fits to the $\log_{10} T_{90}$ variable of 797 GRBs in the BATSE 3B catalog. Several authors (Horváth 2002; Horváth et al. 2008; Horváth 2009; Tarnopolski 2015; Horváth & Tóth 2016; Zitouni et al. 2015; Huja, D. et al. 2009; Modak et al. 2017) have since supported the presence of a third Gaussian component but Zhang et al. (2016) and Kulkarni & Desai (2017) have concluded that the duration variables show a three-Gaussian-components model only for

* E-mail: maitra@iastate.edu (RM)

the *Swift*/BAT dataset but a two-Gaussian-components model for the BATSE and *Fermi* datasets. R pa et al. (2009) analyzed the duration and hardness ratios of 427 GRBs from the RHESSI satellite and found that based on T_{90} a χ^2 - or F -test does not indicate any statistically significant intermediate group in the RHESSI data but a maximum likelihood test using T_{90} and hardness indicates a statistically significant intermediate group in the same data set. They concluded that like BATSE, RHESSI also shows evidence of the presence of an intermediate group. However, use of a χ^2 -test on twice the difference in log likelihoods between two models assumes that the larger model is nested within the null model, an assumption that generally does not hold for non-hierarchical clustering algorithms (Chattopadhyay & Maitra 2017). (Refer to Maitra et al. 2012, for a review of testing mechanisms in such situations.)

Mukherjee et al. (1998) first considered multivariate analysis by carrying out non-parametric hierarchical clustering using six variables on 797 GRBs from the BATSE 3B catalog and found evidence of three groups. They also performed Model Based Clustering (MBC) by eliminating three of those six variables citing presence of redundancy through visual inspection. Chattopadhyay et al. (2007) carried out k -means using the same six variables used by Mukherjee et al. (1998) for non-parametric hierarchical clustering and supported the presence of three groups in the BATSE 4B catalog (but see Chattopadhyay & Maitra 2017, for caution on the use of k -means for BATSE data.) Chattopadhyay & Maitra (2017) carried out model-based variable selection on the six variables used by Chattopadhyay et al. (2007) and Mukherjee et al. (1998) and did not find any evidence of redundancy among them. They carried out MBC using Gaussian mixtures using the same six variables and obtained five homogeneous clusters. The BATSE 4Br catalog has a number of zero entries in some of the observed variables, mostly in the time integrated fluences $F_1 - F_4$. Citing personal communication from Charles Meegan, Chattopadhyay & Maitra (2017) pointed out that these zero values are not numerical zeroes but missing parameter readings on a GRB and hence including them as numerical values in the analysis is inappropriate because of the potential for bias in the results. Most authors performing multivariate analysis have removed those GRBs which have incomplete information in them, as a result of which their properties have never been extensively studied. In this paper we have attempted to study the properties of these bursts having incomplete information by classifying them to groups obtained using GRBs having complete information on all observed variables.

Clustering is an unsupervised learning approach to group observations without any response variable. Numerous clustering algorithms are broadly of two types, that is the hierarchical and the non-hierarchical types. The former consists of both agglomerative and divisive algorithms where groups are formed in a tree-like hierarchy with the property that observations that are together at one level are also together higher up the tree. Non-hierarchical algorithms, such as MBC or k -means, typically optimize an objective function using iterative greedy algorithms for a specified number of groups. The objective function is often multimodal and requires careful initialization (Maitra 2009). For a detailed review on clustering see Chattopadhyay & Maitra (2017).

In this paper, we provide an overview of MBC and clas-

sification using mixtures of multivariate t -distributions that allow for more general model-based representations of elliptical subpopulations than Gaussian mixtures (see Section 2). Section 3 establishes that all nine original parameters have clustering information and analyzes and discusses results on t -mixtures-MBC (t MMBC) done on the 1599 BATSE 4Br GRBs having observations on all nine parameters. Finally Section 3.2 classifies the GRBs having incomplete information to the groups obtained by MBC on the 1599 GRBs and discuss their properties. We conclude with some discussion.

2 OVERVIEW OF MODEL-BASED CLUSTERING AND CLASSIFICATION

We briefly describe t -MMBC and Classification specifically, using that are easily implemented using the open-source statistical software R (R Core Team 2017) and its packages.

2.1 Preliminaries

2.1.1 The Multivariate t distribution

Let Y be a p -dimensional random vector having the multivariate Gaussian distribution $N_p(0, \Sigma)$ and S be a random variable, independent of Y , that has a χ^2 distribution with ν degrees of freedom. Let Σ be positive-definite. Then $X = \mu + Y\sqrt{\nu/S}$ follows a multivariate $t_p(\mu, \sigma; \nu)$ distribution with mean vector μ , scale matrix Σ and degrees of freedom ν , and multivariate probability density function (PDF)

$$f_t(x; \mu, \Sigma, \nu) = \frac{\Gamma(\nu + p)/2}{\Gamma(\nu/2)\nu^{\frac{p}{2}}\pi^{\frac{p}{2}}|\Sigma|^{\frac{1}{2}}}\left[1 + \frac{1}{\nu}(X - \mu)^T \Sigma^{-1}(X - \mu)\right], \quad (1)$$

for $x \in \mathbb{R}^p$. The multivariate t -distribution is centered and ellipsoidally symmetric around its mean vector $E(X) = \mu$. The variance-covariance (or dispersion) matrix is given by $Var(X) = \nu\Sigma/(\nu - 2)$, therefore having higher spread than the $N_p(\mu, \Sigma)$ distribution, with the exact amount of spread modulated by the degrees of freedom ν . It is easy to see that as $\nu \rightarrow \infty$, the dispersion converges to Σ and indeed $t_p(\mu, \sigma; \nu)$ converges in law (distribution) to $N_p(\mu, \Sigma)$. We illustrate the influence of ν through a set of two-dimensional examples in Figure 1 which displays the contour density plot of multivariate t_ν distributions for $\nu = 5, 15, 25, \infty$. The contours are for the ellipses of concentration which contain the densest $100\alpha\%$ of the distribution for $\alpha = 0.1, 0.2, \dots, 0.9, 0.99$. The figure corresponding to $\nu = 5$ has the highest spread, with more observations in the tails, but this spread and tail-preference of the observations decreases with increasing ν . With infinite degrees of freedom, the multivariate t -density has a similar spread as the multivariate normal density. These example illustrate how the multivariate t_ν density is concentrated or dispersed around the mean vector μ accordingly as ν increases or decreases. The $t_p(\mu, \Sigma; \nu)$ distribution has characteristic function as per

Theorem 1. Let X be a p -dimensional random vector having the multivariate t distribution as per (1). Then the char-

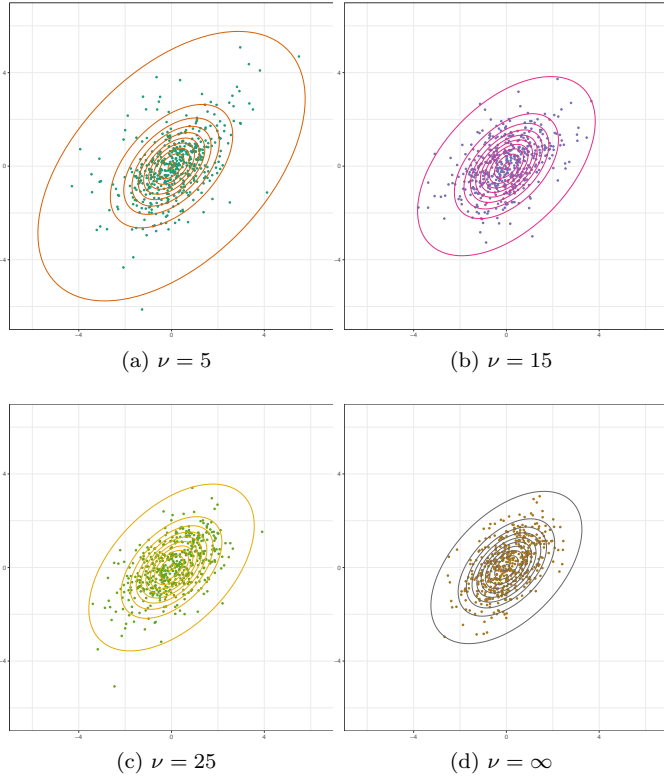


Figure 1. Multivariate $t_\nu(\mu, \Sigma)$ densities and sample realizations for degrees of freedom $\nu = 5, 15, 25$ and ∞ . Here $\mu = (0, 0)$ while Σ is the 2×2 matrix with diagonal entries 1 and off-diagonal elements 0.5.

acteristic function of X is given by

$$\phi_X(t) = \exp(it'\mu) \frac{2}{\Gamma(\frac{\nu}{2})} \left(\frac{ivt'\Sigma t}{4} \right)^{\frac{\nu}{4}} K_{\frac{\nu}{2}}(\sqrt{ivt'\Sigma t}), \quad (2)$$

where $K_{\frac{\nu}{2}}(s)$ is the modified Bessel function of the second kind (Abramowitz & Stegun 1964) of order $\nu/2$ and $\Gamma(z) = \int_0^\infty \exp\{-x\}x^{z-1}dx$ is the gamma function.

Proof. From definitions of the characteristic function of X and the expectation of functions of X , we have $\phi_X(it) = E_X\{\exp(it'X)\} = E_{Y,S}[\exp\{it'(\mu + Y\sqrt{\nu/S})\}] = \exp(it'\mu)E_{Y,S}\{\exp(it'Y\sqrt{\nu/S})\}$. But from the definition of joint expectations, $E_{Y,S}\{\exp(it'Y\sqrt{\nu/S})\} = E_S\{E_{Y|S}[\exp\{it'Y\sqrt{\nu/S}\}]\}$. Also Y is independent of S , so the inner conditional expectation is given by $E_{Y|S}[\exp\{it'Y\sqrt{\nu/S}\}] = \exp\{-ivt'\Sigma t/(2S)\}$. We now use the result (see Bernardo & Smith 1993, pages 119 and 431) that if $S \sim \chi_\nu^2$, then $W = 1/S$ has the inverse- χ_ν^2 distribution with characteristic function given by

$$\phi_W(r) = \frac{2}{\Gamma(\frac{\nu}{2})} \left(-\frac{ir}{2} \right)^{\frac{\nu}{4}} K_{\frac{\nu}{2}}(\sqrt{-2ir}). \quad (3)$$

Then, $E_S[\exp\{-ivt'\Sigma t/(2S)\}]$ is the same as evaluating $\phi_W(r)$ at $r = \nu t'\Sigma t/2$. The theorem follows. \square

Corollary 1. Let X be a p -dimensional random vector from the multivariate t -density $t_p(\mu, \Sigma; \nu)$. Let $X^{(q)}$ be the first $q (\leq p)$ coordinates in X . Then $X^{(q)} \sim t_p(\mu^{(q)}, \Sigma^{(q \times q)}; \nu)$, where $\mu^{(q)}$ is the vector with the first q

coordinates of μ and $\Sigma^{(q \times q)}$ is the $q \times q$ symmetric matrix containing the first q rows and column entries of Σ .

Proof. Setting $t' = (t_1, t_2, \dots, t_q, 0, 0, \dots, 0)$ in (2) yields the characteristic function that is uniquely that of the $t_q(\mu^{(q)}, \Sigma^{(q \times q)}; \nu)$ density and the result follows. \square

2.1.2 Model-based clustering with t -mixtures

MBC is an effective and principled method of obtaining groups of similar observations in a dataset. It scores over partitioning algorithms like k -means mainly in that it is not restricted by the assumption of spherically-dispersed groups. Assuming spherically-dispersed groups when groups are really non-spherical can lead to erroneous results (see Chattopadhyay & Maitra 2017, for a comprehensive review on the pitfalls of using k -means when assumptions are not met.) In MBC (Melnikov & Maitra 2010; McLachlan & Peel 2000; Fraley & Raftery 2002a) the observations X_1, X_2, \dots, X_n are assumed to be realizations from a K -component mixture model (McLachlan & Peel 2000) with PDF

$$f(x; \theta) = \sum_{k=1}^K \pi_k f_k(x; \eta_k) \quad (4)$$

where $f_k(\cdot; \eta_k)$ is the density of the k th group, η_k the vector of unknown parameters and $\pi_k = Pr[x_i \in G_k]$ is the mixing proportion of the k th group, $k = 1, 2, \dots, K$, and $\sum_{k=1}^K \pi_k = 1$. For convenience, we write θ as the set of all the model parameters. The most popular mixture model is the Gaussian Mixture Model (GMM) where the component densities are assumed to be multivariate Gaussian $\phi(x; \mu_k, \Sigma_k)$ with mean μ_k and dispersion Σ_k . Imposing different constraints on the densities (mostly on the dispersion matrices) gives rise to a family of mixture models that are more parsimonious compared to the fully unconstrained model. The popular GMM family (MCLUST) of Fraley & Raftery (1998, 2002a) uses an eigen-decomposition of the component's variance covariance matrices. Thus, they write $\Sigma_k = \lambda_k B_k \Lambda_k B_k^T$, where Λ_k is a diagonal matrix with values proportional to the eigen values of Σ_k , B_k denotes the matrix of eigen vectors of Σ_k and λ_k is the constant of proportionality. The MCLUST family (Fraley & Raftery 1998, 2002a) has 17 GMMs obtained by imposing certain constraints on λ_k , B_k and Λ_k and is implemented using the R (R Core Team 2017) package `mclust` (Fraley & Raftery 2002b; Fraley et al. 2012). Another useful class of mixture models is obtained when the component cluster densities are assumed to follow a multivariate t -distribution rather than a multivariate Gaussian distribution. Motivated by McLachlan & Peel (1998), these mixture models perform better than GMM when it is plausible for each group has some extreme observations. Andrews & McNicholas (2012) proposed a set of multivariate t mixture models (t MM) by imposing the same constraints as MCLUST plus additional constraints on ν to provide 24 multivariate t MMs. These models are implemented in the `teigen` package (Andrews & McNicholas 2015) in R (R Core Team 2017).

The most common method of estimating the parameters of a mixture model is the Expectation Maximization (EM) Algorithm (Dempster et al. 1977; McLachlan & Krishnan 2008), which is an iterative method for finding maximum

likelihood estimates (MLEs) in incomplete data setup. Andrews & McNicholas (2012) used a variant of EM known as the Expectation Conditional Maximization (ECM) algorithm (Meng & Rubin 1993) to estimate the parameters of the *tMM*. Faster modifications (Meng & Van Dyk 1997; Chen & Maitra 2011) exist but they have the same idea as ECM, in that they replace the M-step of EM with a sequence of D Conditional Maximization (CM) steps. Thus, the vector of parameters θ is partitioned into D sub-vectors $\theta = (\theta_1, \theta_2, \dots, \theta_D)$ and the maximization done in D steps, where the d th CM step maximizes the Q function (or the expected complete log likelihood function given the observations) over θ_d but while keeping the other sub-vectors fixed at some previous value. ECM is computationally more efficient than EM and also shares its desirable convergence properties (Meng & Rubin 1993). We now outline ECM estimation in the context of *tMMs*.

Let ζ_{ik} be indicator variables that denote the cluster membership of the i th observation. Thus

$$\zeta_{ik} = \begin{cases} 1, & \text{if the } i\text{th observation } x_i \text{ belongs to the } k\text{th group} \\ 0, & \text{otherwise.} \end{cases} \quad (5)$$

Note that ζ_{iks} are unobserved and estimating them is the major objective of MBC. In the context of the *tMM*, there is an additional set of missing values $v_{ik}, i = 1, 2, \dots, n; k = 1, 2, \dots, K$ which are realizations from the Gamma density with PDF

$$\gamma(v_{ik}; \nu_k/2, \nu_k/2) = \frac{\nu_k^{\frac{\nu_k}{2}} v_{ik}^{\frac{\nu_k}{2}-1} \exp(-\frac{\nu_k v_{ik}}{2})}{2^{\frac{\nu_k}{2}} \Gamma(\frac{\nu_k}{2})}. \quad (6)$$

The for the *tMM* the complete data loglikelihood can be written as

$$\begin{aligned} \ell(\pi, \mu, \Sigma, \zeta) \\ = \sum_{k=1}^K \sum_{i=1}^n \zeta_{ik} \log \{ \pi_k \phi(x_i; \mu_k, \Sigma_k/v_{ik}) \gamma(v_{ik}; \nu_k/2, \nu_k/2) \} \end{aligned} \quad (7)$$

where ν_k denotes the degrees of freedom of the t density for the k th group, ϕ denotes Gaussian density with mean μ_k and variance Σ_k/v_{ik} . The *tMM* likelihood is maximized through the following steps:

(i) *Initialization*. Let $\{(\pi_k^\circ, \mu_k^\circ, \Sigma_k^\circ, \nu_k^\circ); k = 1, 2, \dots, K\}$ be the initializing parameters.

(ii) *E-step updates*. The component weights v_{ik} and the group indicator variables ζ_{ik} are updated as

$$\begin{aligned} \hat{v}_{ik} &= \frac{\nu_k^\circ + p}{\nu_k^\circ + (x_i - \mu_k^\circ)^T \Sigma_k^{\circ-1} (x_i - \mu_k^\circ)} \\ \hat{\zeta}_{ik} &= \frac{\pi_k^\circ f_t(x_i; \mu_k^\circ, \Sigma_k^\circ, \nu_k^\circ)}{\sum_{k=1}^K \pi_k^\circ f_t(x_i; \mu_k^\circ, \Sigma_k^\circ, \nu_k^\circ)} \end{aligned}$$

where $f_t(x_i; \mu_k^\circ, \Sigma_k^\circ, \nu_k^\circ)$ denotes a multivariate t -density with mean μ_k , dispersion matrix Σ_k and degrees of freedom ν_k .

(iii) *CM-step 1*. The first CM step updates the component

means μ_k s and the prior probabilities π_k s:

$$\begin{aligned} \hat{\pi}_k &= \frac{\hat{n}_k}{n} \\ \hat{\mu}_k &= \frac{\sum_{i=1}^n \hat{\zeta}_{ik} \hat{v}_{ik} x_i}{\sum_{i=1}^n \hat{\zeta}_{ik} \hat{v}_{ik}} \end{aligned}$$

where $\hat{n}_k = \sum_{i=1}^n \hat{\zeta}_{ik}$. Additionally, if the constraint $\nu_k = \nu$ is imposed upon the degrees of freedom of each group, then $\hat{\nu}$ is updated here by solving the equation

$$\begin{aligned} 1 - \psi\left(\frac{\hat{\nu}}{2}\right) + \frac{1}{n} \sum_{k=1}^K \sum_{i=1}^n \hat{\zeta}_{ik} (\log \hat{v}_{ik} - \hat{v}_{ik}) + \log\left(\frac{\nu}{2}\right) \\ + \psi\left(\frac{\nu^\circ + p}{2}\right) - \log\left(\frac{\nu^\circ + p}{2}\right) = 0. \end{aligned} \quad (8)$$

where $\hat{\nu}$ denotes the updated degrees of freedom and ν° denotes the current estimate.

(iv) *CM-step 2*. This step updates the Σ_k s and varies accordingly as per constraints imposed in the modeling. For example, if we set $\Lambda_k = \Lambda$ and $B_k = B$ yields the updates

$$\hat{\lambda}_k = \frac{1}{p \hat{n}_k} \text{trace}(S_k H^{-1}) \quad (9)$$

where $S_k = \frac{1}{\hat{n}_k} \sum_{i=1}^n \hat{\zeta}_{ik} \hat{v}_{ik} \|x_i - \hat{\mu}_k\|^2$ and $H = B \Lambda B^T$. In order to update B and Λ , H is first updated using using

$$H = \frac{\frac{1}{\lambda_k} \sum_{k=1}^K S_k}{\left| \frac{1}{\lambda_k} \sum_{k=1}^K S_k \right|^{\frac{1}{p}}} \quad (10)$$

Now the updated B and Λ are obtained from (10).

(v) Alternate between the E- and CM-steps till convergence.

After obtaining the final estimates of the parameters, the i th data point X_i is assigned to the class for which the converged E-step posterior probability is the highest that is X_i is assigned to class k where $k = \arg \max_l \hat{\zeta}_{il}$.

Our *t*-mixtures MBC (*t*-MMBC) formulation above assumes a known number of components K . With unknown K , a popular approach of finding it is the Bayesian Information Criterion (BIC) (Schwarz 1978) which subtracts $(m \log n)/2$ from the maximized log-likelihood (obtained from the converged ECM), with m the number of unconstrained parameters in the fitted K -component *tMM*. (See Chattopadhyay & Maitra 2017, for a detailed review of BIC.)

2.1.3 Illustration

The purpose of this section is to demonstrate using a simulated dataset, potential pitfalls in fitting a GMM on data that are plausibly realizations from a multivariate *tMM*. For this purpose, we simulated three 4-component multivariate *tMMs* having an approximate generalized overlap (Maitra 2010; Melnykov & Maitra 2011) of $\tilde{\omega} = 0.01$ and $\nu = 5, 15, 25$ degrees of freedom. The generalized overlap measure is an effective way of summarizing the overlap matrix Ω of Maitra & Melnykov (2010) which is a $K \times K$ matrix whose (i, j) th element contains the sum of misclassification probabilities between i th and j th clusters. The generalized overlap summarizes this matrix and is defined as $\tilde{\omega} = (\lambda_{(1)} - 1)/(K - 1)$ where $\lambda_{(1)}$ is the largest eigen value of Ω . Small values of $\tilde{\omega}$ are likely to indicate more distinct groupings. (See also

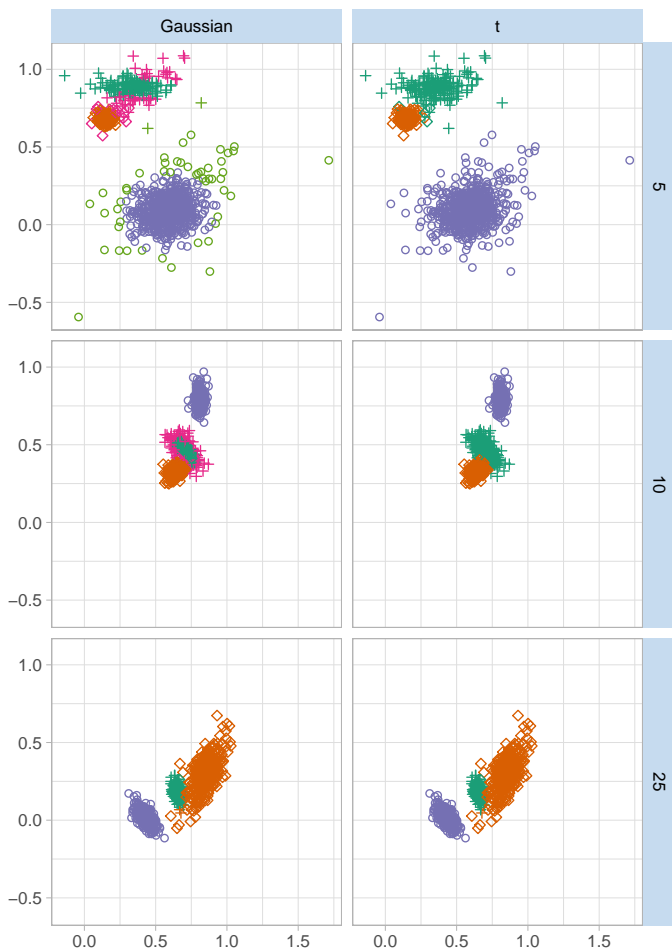


Figure 2. Simulated datasets from a bivariate tMM with $\nu = 5, 10, 25$ in the top, middle and bottom panels, and clustering obtained using GMM (left panel) and tMM (right panel). In all figures, plotting character indicates true classification while color indicates estimated grouping.

Chattopadhyay & Maitra 2017, for further details.). The `MixGOM()` function in the R package `MixSim` (Melnykov et al. 2012) can be adapted in the same manner as Melnykov & Maitra (2011) to obtain realizations from a multivariate tMM with a specified $\tilde{\omega}$.

We fitted both GMM and tMM to the datasets, with optimal number of groups determined using BIC, and results displayed in Figure 2. For $\nu = 5$ and $\nu = 10$ fitting a GMM we get the optimal number of clusters to be 5 and 4 respectively but for tMM the optimum number of clusters were correctly chosen as 3 in both cases. For $\nu = 25$, BIC identified the number of clusters as 3 for both class of models.

For numerical assessment of clustering performance, we computed the Adjusted Rand Index (\mathcal{R}) after fitting each of the two models to the data. As also explained by Maitra (2001), the Rand Index (Rand 1971) is a measure of similarity between two different clusterings and is calculated as follows. Suppose that for a given data set \mathcal{D} having n elements there exists two different partitions P_1 and P_2 by two different algorithms. Let a_1 denote the number of pairs of object in \mathcal{D} that are in the same group in both the partitions P_1 and P_2 and a_2 the number of pairs of objects in \mathcal{D}

Table 1. Adjusted Rand Indices obtained by clustering three datasets simulated from a 3-component tMM with ν equal to 5, 10 and 25 using a Gaussian mixture model and a t mixture model.

ν	Gaussian	t
5	0.84	0.99
10	0.79	0.99
25	0.99	0.99

that are in different groups in both the partitions P_1 and P_2 . Then the Rand Index is defined as $(a_1 + a_2) / \binom{n}{2}$. The Rand Index takes values between 0 and 1. The Adjusted Rand Index (Hubert & Arabie 1985) is obtained by correcting Rand Index for chance grouping of elements and can take values between $-\infty$ and 1. We analyzed the quality of clustering for both GMM and tMM by comparing the clustering results with the true class indicators through \mathcal{R} in order to demonstrate issues of using a GMM model for clustering a data supposedly originating from a tMM , that is from a mixture model with potentially heavier tails. The results are presented in Table 1. Both Figure 2 and Table 1 clearly indicate that a tMM gives a better fit than a GMM , with the most notable difference observed for $\nu = 10$. For $\nu = 25$ the difference is negligible but enough to prove that tMM wins over GMM . Our examples here illustrate the value of considering a tMM when the underlying groups are potentially thicker-tailed.

2.2 Variable Selection in Clustering

Selection of relevant variables is a very important issue in clustering. Incorporating redundant information degrades overall clustering performance less distinct groups (Chattopadhyay & Maitra 2017). In the same way exclusion of variables having relevant information also degrades the overall quality of clustering. We illustrate this problem by means of a simulated three-dimensional dataset drawn from a GMM with $K = 6$ true components and having means $(1,0,0)$, $(0,1,0)$, $(0,0,1)$, $(1,1,0)$, $(1,0,1)$, $(0,1,1)$ respectively and the same variance-covariance matrix (that is 0.125 on the diagonals and 0.1 on the off-diagonals). We group this dataset using each of the three sets of bivariate pairs of variables and using GMMBC. Figures 3a, 3b and 3c display the results and show that no matter which of the pairs of coordinates is selected, it is not possible to identify the six groups. This is because upon dropping a variable, two groups become indistinguishable in each case. The degradation in the clustering due to this loss of coordinate information is also clearly visible in Figures 3a, 3b and 3c where different characters represent the original grouping and different colors represent the clustering obtained. On the other hand, when all the coordinates are considered, then the six groups are correctly identified (Figure 3d) with $\mathcal{R} = 1$. Therefore, it is important to consider the relevant variables in astronomy. This fact becomes more important in the light of attempts by many researchers to cluster GRBs using, for instance, only the duration variables. Raftery & Dean (2006) proposed a method for selecting variables containing the most relevant clustering information by recasting the variable selection problem in terms of model selection, where compari-

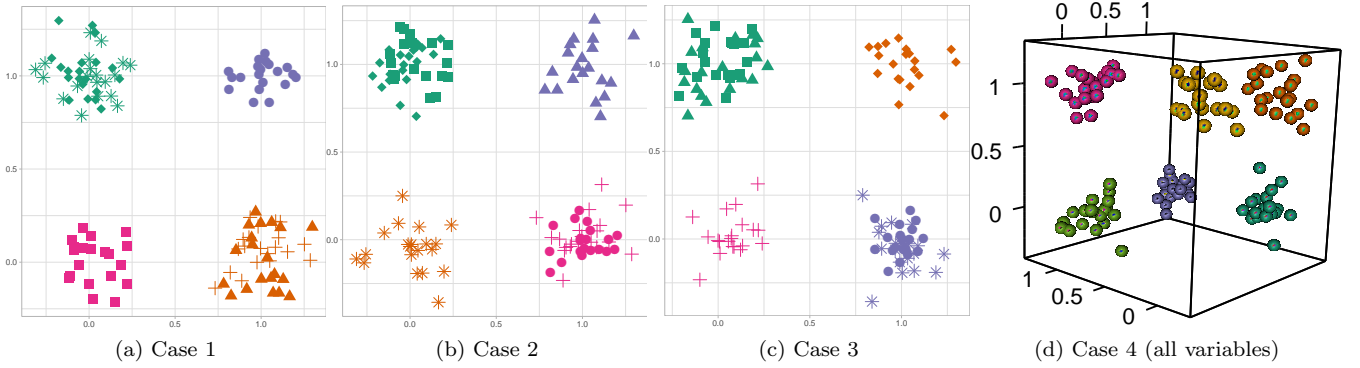


Figure 3. Results of Clustering data from 3 dimensional 6 component GMM using two (a, b and c) and three variates.

son of the models is done via BIC. (Refer to Chattopadhyay & Maitra 2017, for a thorough review on variable selection.)

2.3 Classification

The objective of classification is to classify a new observation to one of K well-defined groups. Classification is a supervised learning method that uses training data to determine a rule that classifies a new observation to one of K groups. Bayes' rule is often used to obtain classification rules in the model-based context. Here an observation x is assigned to the l th group if the posterior probability of x belonging to the i th group is highest among all groups under considerations. Thus, the decision rule is to classify x to group i if $\pi_i f_i(x) > \pi_k f_k(x)$ for all $k \neq i$, where π_j is the prior probability that an observation belongs to the j th group and $f_j(x)$ denotes the probability density of the j th group at x . In case of tMM $f_i(x)$ denotes a multivariate t density and π_i the prior probability of an observation belonging to the i th group. (See Johnson & Wichern 1988, for more details.) Our proposal is to cluster the observations for which all parameters are observed and to use the estimated parameters to classify the GRBs for which not all parameters are observed. We will use the above methods for developing our classification rule.

3 CLUSTER ANALYSIS OF GRBS

The BATSE catalogue is widely used for analysis of GRBs and has temporal and spectral information of GRBs from 1991 to 2000. A few of the parameters have been of interest to researchers for grouping GRBs. These are:

- T_{50} : The time by which 50% of the flux arrive.
- T_{90} : The time by which 90% of the flux arrive.
- $P_{64}, P_{256}, P_{1024}$: The peak fluxes measured in bins of 64, 256 and 1024 milliseconds, respectively.
- F_1, F_2, F_3, F_4 : The four time-integrated fluences in the 20-50, 50-100, 100-300, and > 300 keV spectral channels, respectively.

Apart from these nine parameters three more composite parameters are of interest to researchers (Mukherjee et al. 1998). These are:

$F_t = F_1 + F_2 + F_3 + F_4$: The total fluence of a GRB.

$H_{32} = F_3/F_2$: Measure of spectral hardness using the ratio of F_2 and F_3 .

$H_{321} = F_3/(F_1 + F_2)$: Measure of spectral hardness based on the ratio of channel fluences F_1, F_2, F_3 .

The current (BATSE 4Br) catalogue contains revised locations of 208 bursts from the BATSE 4B Catalog along with 515 bursts observed between 20 September 1994 and 29 August 1996 apart from the bursts present in the BATSE 3B Catalog. Many parameters, especially in the four time-integrated fluences F_1, F_2, F_3 and F_4 are missing (Chattopadhyay & Maitra 2017). Consequently, the derived variables are also missing for these GRBs. On account of this reason the BATSE 4Br catalog has 1599 GRBs (among 1973 GRBs) containing complete information on all the nine original (plus three derived) variables. Most authors have used a very subset of these 12 variables for their analysis. This led us to wonder whether the nine original variables contains relevant information which might improve the quality of clustering to give more coherent groups. We thus analyze 1599 GRBs from the BATSE 4Br catalog having complete information on the nine original variables with MBC using mixtures of t densities. Further, we wondered if the 5 groups identified by Chattopadhyay & Maitra (2017) were only because the groups identified were Gaussian and so had thinner tails, while in reality, we had fewer groups with thicker tails in a scenario reminiscent of the situation in Figure 2. Therefore, we reanalyzed the BATSE data using all nine parameters and tMMBC.

We first briefly discuss the univariate and bivariate relationships between the nine original parameters in the BATSE 4Br catalog. Figure 4 displays the bivariate relationships between the nine original variables of the BATSE 4Br catalogue along with the univariate density plots of the nine parameters. The two duration variables $\log_{10} T_{50}$ and $\log_{10} T_{90}$ exhibit a very high positive association amongst themselves. Similar behavior is exhibited by the three peak fluxes $\log_{10} P_{64}, \log_{10} P_{256}$ and $\log_{10} P_{1024}$. Fluence $\log_{10} F_1$ shows a very high positive association with fluences $\log_{10} F_2$ and $\log_{10} F_3$ and a high positive association with $\log_{10} F_4$. Fluence $\log_{10} F_2$ exhibits a very high positive association with $\log_{10} F_3$ and a high positive association with $\log_{10} F_4$ which also shows a high positive association with $\log_{10} F_3$. Duration $\log_{10} T_{50}$ exhibits a high positive association with

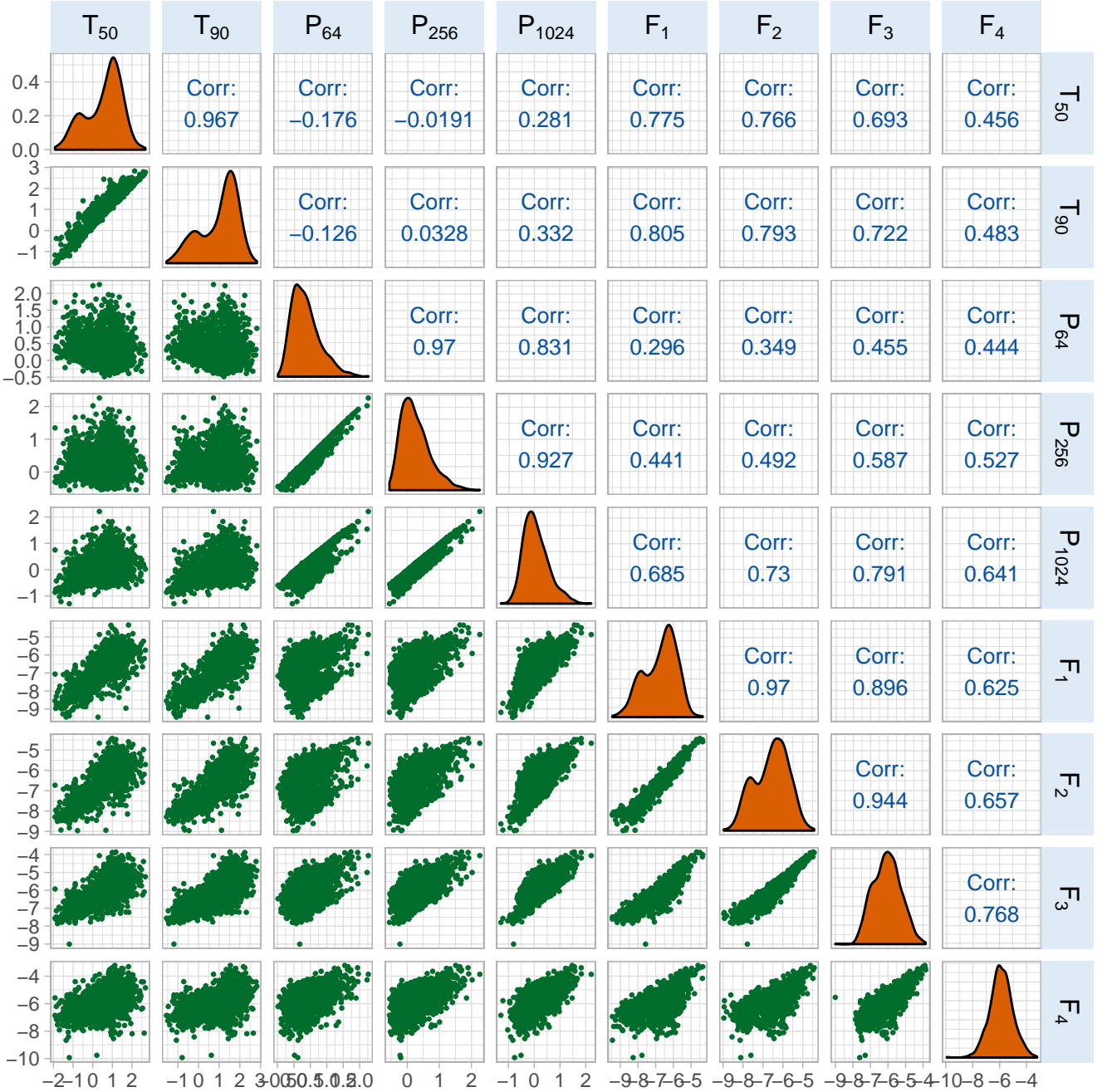


Figure 4. A matrix of scatterplots (the lower triangular portion), density plots (the diagonal) and correlation coefficients (the upper triangular portion) of the nine parameters T_{50} , T_{90} , P_{64} , P_{256} , P_{1024} , F_1 , F_2 , F_3 and F_4 using 1599 GRBs of the BATSE 4Br catalogue. All displays are in the logarithmic scale.

fluences $\log_{10} F_1$, $\log_{10} F_2$ and $\log_{10} F_3$ and a moderate positive association with $\log_{10} F_4$. $\log_{10} T_{90}$ behaves similar to $\log_{10} T_{50}$ except that it shows a very high positive association with $\log_{10} F_1$. Figure 3 and Chattopadhyay & Maitra (2017) has also pointed out through the scatterplots the limitations that are posed on grouping using only one or two variables, thus pointing out the importance of using more than two variables for clustering. We now perform cluster analysis on the 1599 GRBs using the nine original parameters

(in logarithmic scale) $\log_{10} T_{50}$, $\log_{10} T_{90}$, $\log_{10} F_1$, $\log_{10} F_2$, $\log_{10} F_3$, $\log_{10} F_4$, $\log_{10} P_{64}$, $\log_{10} P_{256}$ and $\log_{10} P_{1024}$.

3.1 Clustering GRBs Using All Observed Parameters

We first perform *t*MMBC using 1599 GRBs from the BATSE 4Br catalogue and then classify the GRBs with incomplete information to the groups obtained using the *t*MMBC.

Table 2. Results of forward- and backward-variable selection for determining redundancy among $\log_{10} T_{90}$, $\log_{10} T_{50}$, $\log_{10} P_{64}$, $\log_{10} P_{1024}$, $\log_{10} P_{256}$, $\log_{10} F_3$, $\log_{10} F_2$, $\log_{10} F_1$, $\log_{10} F_4$ for MBC.

Step	Variable	Step Type	BIC Difference	Decision
1	$\log_{10} T_{90}$	Add	452.95	Accepted
2	$\log_{10} T_{50}$	Add	395.74	Accepted
3	$\log_{10} P_{64}$	Add	181.35	Accepted
4	$\log_{10} P_{64}$	Remove	181.73	Rejected
5	$\log_{10} P_{1024}$	Add	1636.98	Accepted
6	$\log_{10} T_{90}$	Remove	391.06	Rejected
7	$\log_{10} P_{256}$	Add	1266.77	Accepted
8	$\log_{10} T_{90}$	Remove	235.84	Rejected
9	$\log_{10} F_3$	Add	540.03	Accepted
10	$\log_{10} T_{90}$	Remove	243.47	Rejected
11	$\log_{10} F_2$	Add	509.78	Accepted
12	$\log_{10} T_{90}$	Remove	95.59	Rejected
13	$\log_{10} F_1$	Add	312.38	Accepted
14	$\log_{10} T_{90}$	Remove	45.00	Rejected
15	$\log_{10} F_4$	Add	113.55	Accepted
16	$\log_{10} F_4$	Remove	16.09	Rejected

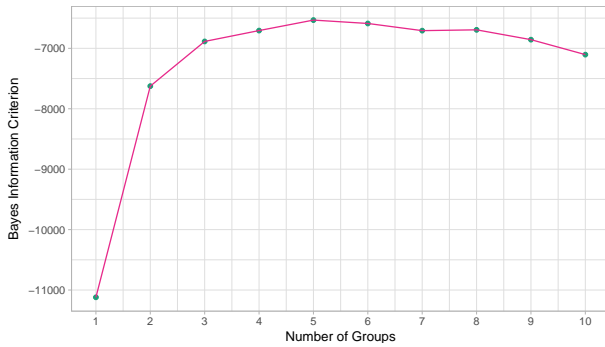


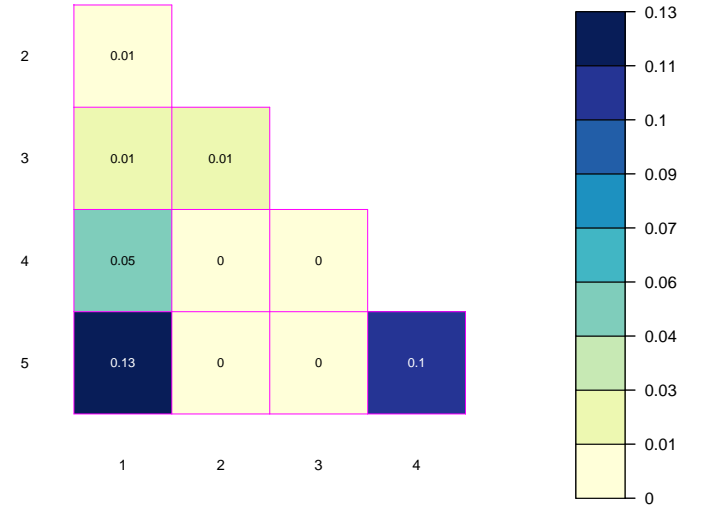
Figure 5. Plot of BIC with K upon performing t MMBC of the 1599 GRBs in the BATSE 4Br catalogue.

3.1.1 t MMBC with all nine parameters

We first check for the presence of redundancy for clustering amongst the nine original variables $\log_{10} T_{50}$, $\log_{10} T_{90}$, $\log_{10} P_{64}$, $\log_{10} P_{256}$, $\log_{10} P_{1024}$, $\log_{10} F_1$, $\log_{10} F_2$, $\log_{10} F_3$, $\log_{10} F_4$ using model-based variable selection. The results obtained (Table 2) does not show much support towards the presence of redundancy amongst the nine original variables. However, there is redundancy beyond these nine variables, because the derived variables are linearly related to the nine parameters. We thus performed t MMBC on the nine original variables using the `teigen` package in R and determined K from among $\{1, 2, \dots, 9\}$ using BIC – indeed, Figure 5 indicates overwhelming evidence in favor of a 5-component t MM, with a difference of greater than 10 than for other K , which as per Kass & Raftery (1995), constitutes very strong evidence. The results obtained mirror those of Chattopadhyay & Maitra (2017) which also found 5 groups upon performing GMMBC.

3.1.1.1 Validity of obtained groupings The overlap measure of Melnykov & Maitra (2011) can be used to analyze the distinctiveness of the groups obtained through clus-

Figure 6. Pairwise overlap measures between the k th and the l th groups obtained by our 5-component t MMBC solutions.



tering. The overlap measure between two Gaussian groups is defined as the sum of their misclassification probabilities (Melnykov & Maitra 2011). (See Chattopadhyay & Maitra 2017, for further details.) However, the computations in the MixSIM package (Melnykov et al. 2012) are for Gaussian components so we follow the suggestion of (Melnykov & Maitra 2011) in transforming the scale matrices of the t MM components into dispersion matrices and calculating an approximate overlap measure. The overlap map of Figure 6 shows the distinctness of the five groups obtained using t MMBC. It is evident that the Group 4 has a very small overlap with both Groups 2 and 3 and so does Group 5. However, Groups 1 and 5 have the highest overlap while the pairwise overlap measures between Groups 1, 2 and 3 are moderate. The overlap map indicates that the clusters obtained are quite well-separated and so our results provide five more distinct GRB subpopulations than Chattopadhyay & Maitra (2017) using all the observed variables. Apart from this the generalized overlap (see Chattopadhyay & Maitra (2017)) for the five component solutions is 0.05 which is much less than the five component GMMBC solution obtained by Chattopadhyay & Maitra (2017) (0.10) which adds support towards the fact the groups obtained here are more distinct than those obtained by Chattopadhyay & Maitra (2017).

3.1.1.2 Analysis of Results Table 4a provides the number of observations in each group, with the color for the group indicators matching the color of the groups in all figures to provide for easy cross-referencing. We see that Groups 1 and 5 contains the highest number of GRBs while Group 3 contains the lowest number of GRBs. Table 4b also lists the means of the five groups. A more detailed visual representation is provided by Figure 7 which displays the five groups via a parallel coordinate plot (Inselberg 1985; Wegman 1990) that was introduced in the astronomy literature by Chattopadhyay & Maitra (2017).

To study the properties of the five groups obtained we take a closer look at the duration variable $\log_{10} T_{90}$. This variable also facilitates comparison of our results to the

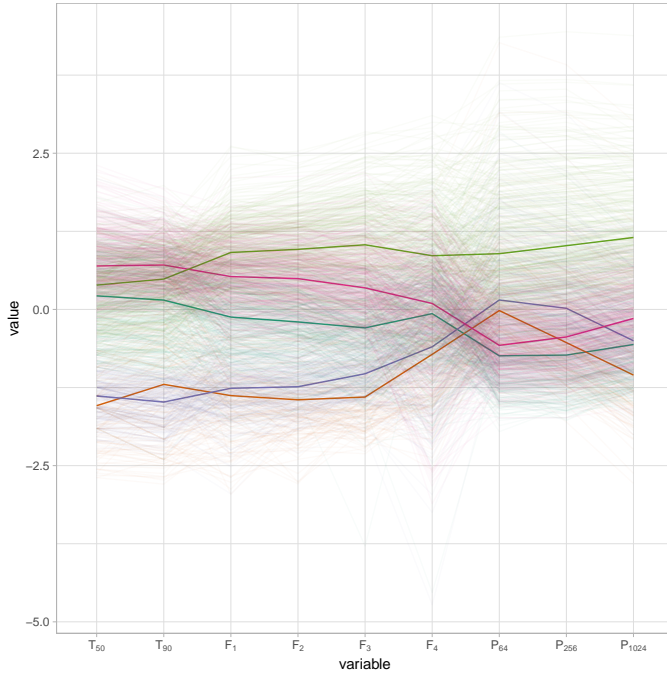
Table 3. (a) Number of GRBs and (b) group means of the nine parameters in each of the five groups obtained using *t*MMBC.

Group	1	2	3	4	5
Number of observations	461	239	161	324	414

(a) Number of observations in each group

k	$\log T_{50}$	$\log T_{90}$	$\log F_1$	$\log F_2$	$\log F_3$	$\log F_4$	$\log P_{64}$	$\log P_{256}$	$\log P_{1024}$
1	0.74	1.13	-6.83	-6.72	-6.27	-5.96	0.10	-0.01	-0.15
2	-0.73	-0.36	-7.90	-7.60	-6.81	-6.42	0.49	0.32	-0.12
3	-0.68	-0.13	-7.98	-7.76	-7.06	-6.49	0.43	0.13	-0.35
4	0.91	1.45	-5.92	-5.77	-5.28	-5.17	0.77	0.74	0.65
5	1.22	1.64	-6.24	-6.15	-5.75	-5.81	0.15	0.09	0.03

(b) Mean parameter values for each group

**Figure 7.** Parallel coordinate plot of the 1599 BATSE 4Br GRBs colored as per their group indicators. The solid lines represent the group medians for each of the nine variables displayed. Variables are in the logarithmic scale.

results obtained by Chattopadhyay & Maitra (2017) and other authors such as Mukherjee et al. (1998) who have used $\log_{10} T_{90}$ along with other derived variables such as $\log_{10} F_t$. Our fourth and fifth group contains the bursts of highest duration (around 28s and 44s respectively). Typically the bursts from these two groups and the first group are designated as long duration bursts ($T_{90} > 2s$) following the popular classification scheme of classifying bursts with duration less than 2s as short duration bursts and bursts greater than 2s as long duration bursts (Chattopadhyay et al. 2007). The second and third groups consist of bursts of shortest duration (around 0.4s and 0.7s respectively) and will be classified as short duration bursts ($T_{90} < 2s$). The

Table 4. Number of 1599 GRBs assigned to each of the groupings by *t*MMBC using the nine original variables (Grouping I) and GMMBC of Chattopadhyay & Maitra (2017) using three original variables ($\log_{10} T_{50}$, $\log_{10} T_{90}$, $\log_{10} P_{256}$) and three derived variables $\log_{10} F_t$, $\log_{10} H_{32}$, $\log_{10} H_{321}$.

		Grouping I (New groupings)					Total
		1	2	3	4	5	
Grouping II	1	86	50	14	24	0	174
	2	5	57	25	2	60	149
	3	45	48	198	0	1	292
	4	186	5	0	319	41	551
	5	38	0	0	134	261	433
Total		60	160	237	479	363	

long GRBs in Groups 4 and 5 have high fluence in all the four channels compared to the short GRBs. Typically bursts in Group 4 have the highest fluence compared to the bursts in first and fifth groups. Hence one can designate the GRBs in the fourth group as long duration high fluence bursts while those of Group 1 are the duration low fluence bursts. Bursts in Groups 2 and 3 have bursts of lowest fluences. In fact, the mean of $\log_{10} T_{90}$ for Group 2 shows resemblance to the mean of Group 4 obtained by Chattopadhyay & Maitra (2017) for $\log_{10} T_{90}$ (around 0.4s). Our fifth group contains bursts of highest duration and largest fluences which mirrors the result of Chattopadhyay & Maitra (2017) whose fifth group contained GRBs with longest duration and highest total fluence. One can thus infer from the results that generally bursts of longer duration typically have high fluences compared to bursts to lower duration – a claim also supported by many researchers.

Additionally we compared our *t*MMBC grouping with the GMMBC grouping of Chattopadhyay & Maitra (2017) by means of a cross classification table (Table 4). The high values in the diagonal (with the exception for Group 2) indicates that the grouping structure in both the cases agrees well for both the analyses with the highest agreement being noted in the Group 4.

In order to facilitate further study of the group structures we calculated the correlations between the nine classes for each of the five groups (Figure 8). The diagonals of each

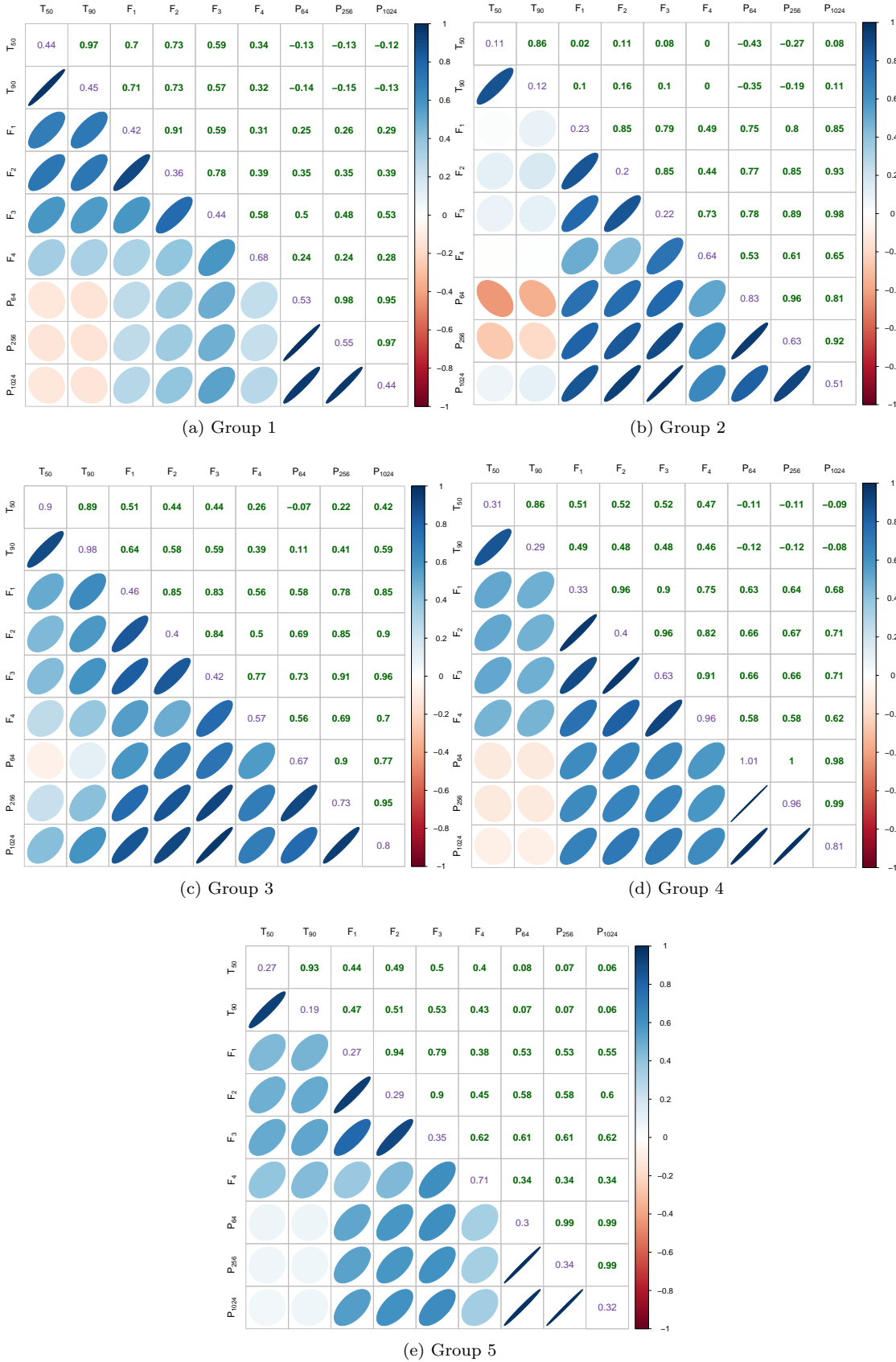


Figure 8. Variances and displays of the estimated correlations for each of the five groups obtained from the 5-component MBC solution using t mixtures for the 1599 GRBs. For each group, the off-diagonal elements display correlation between the variables while the diagonals display the variances. Both correlations and variances are calculated for the variables in the base-10 logarithmic scale.

of the correlation plots display the estimated variance of the five groups obtained by *t*MMBC. The upper triangular portion of each correlation plot displays the correlation between the variables while the lower triangular part provides a diagrammatic representation of the correlations in the upper triangular part (For example, the (2,1)th cell displays the correlation between $\log_{10} T_{50}$ and $\log_{10} T_{90}$ diagrammatically while the (1,2)th cell displays the numerical value). The duration variables $\log_{10} T_{50}$ and $\log_{10} T_{90}$ display very high positive association in all five groups. Duration $\log_{10} T_{50}$ and fluence $\log_{10} F_1$ have moderately positive association in Groups 1, 3 and 4 and a high positive association in Group 5. In Group 2, they have very low positive association. The other fluences $\log_{10} F_2$, $\log_{10} F_3$ and $\log_{10} F_4$ also exhibit similar linear relationships with $\log_{10} T_{50}$ for the five groups. Duration $\log_{10} T_{90}$ has moderately positive association with $\log_{10} F_1$ in Groups 1 and 4 and a strong positive association in Groups 3 and 5. The association between them is weak in Group 2. Also, $\log_{10} T_{90}$ displays a moderately positive association with fluence $\log_{10} F_2$ in Group 4 and high positive association in Groups 1 3 and 5. In Group 2, they display a low positive association. Fluence $\log_{10} F_4$ exhibits a moderate positive association with $\log_{10} T_{90}$ in Groups 1, 3 and 4 and a weak positive association in Group 5. They have a very weak positive association in Group 2. Fluences $\log_{10} F_1$ and $\log_{10} F_2$ show very high positive association in all five groups. $\log_{10} F_2$ and $\log_{10} F_3$ has a very strong positive association in Groups 1, 2 3 and 4 while in Group 5 they have a strong positive association. Fluence $\log_{10} F_4$ has a moderate positive association with $\log_{10} F_1$ in Groups 1, 2 and 3 and a strong positive association in Group 4. In Group 5 they exhibit a weak positive association. Peak flux $\log_{10} P_{64}$ and $\log_{10} T_{90}$ have weak positive association in Group 1 and 3, a moderately negative association in Group 2 and a weak negative association in Groups 4 and 5. These correlations once again support the hypothesis that the total amount of fluence in higher duration bursts are likely to more compared to that of shorter duration bursts.

Our analysis so far has been on 1599 GRBs for which observations are available for all nine parameters. We now use the results of our *t*MMBC on 1599 GRBs to classify the 374 BATSE GRBs with incomplete observations.

3.2 Classification of 374 GRBs with partially observed parameters

There are 374 GRBs in the BATSE catalogue with incomplete information in one or more parameters (mainly in the four fluences $F_1 - F_4$), as seen in Table 5 which enumerates the number of GRBs having incomplete information in the nine observed parameters. In Section 3.1 we excluded these GRBs from multivariate analysis since standard MBC techniques are not suited to address situations with missing variables. Here, we illustrate how we can use the clustering results of Section 3.1 along with classification methods of Section 2.3 to group the GRBs with missing parameters. We first develop some methodology for this purpose.

Corollary 1 implies that excluding the parameters that are missing for a GRB yields an observation of reduced dimensions that still has a multivariate *t* distribution with parameters corresponding to the coordinates that are observed. Therefore the classification rule of Section 2.3 can

Table 5. Number (n_j) of observations with incomplete information in each of the BATSE 4Br catalogue parameters (denoted by X_j).

X_j	T_{50}	T_{90}	P_{64}	P_{256}	P_{1024}	F_1	F_2	F_3	F_4
n_j	0	0	1	1	1	29	12	6	339

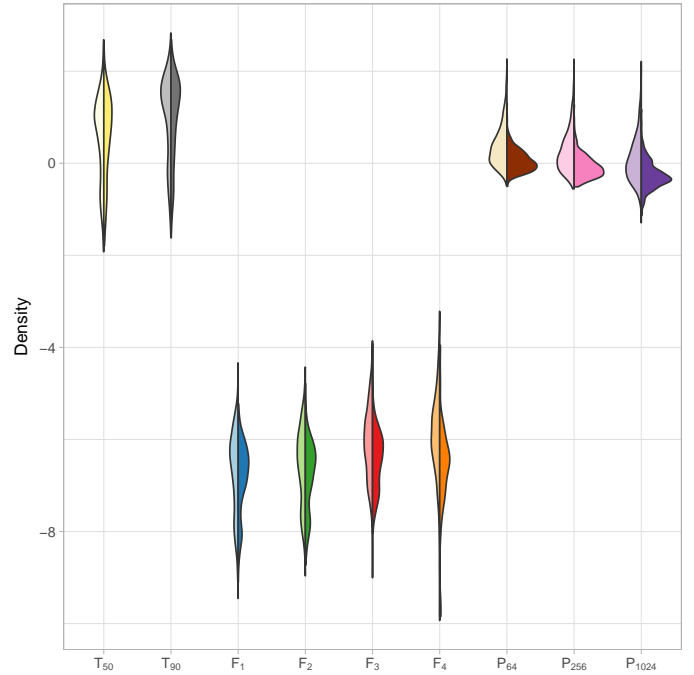


Figure 9. Split violin plot of the nine observed variables where the left side of each violin is the kernel density estimate of the 1599 GRBs with complete information and the right side is the kernel density estimate of the 374 GRBs with incomplete information.

still be used with the density f_i s in that discussion the same as the reduced t_ν density as per Corollary 1. Therefore, the parameter estimates returned by *t*MMBC as per our ECM algorithm of 2.1 can be used. Specifically, the estimated μ_k s are used, but only the coordinates that are observed for the GRB under consideration are included in the calculation of the classification rule. Similarly, only the rows and columns of Σ_k s that are observed are included in the classification rule. The estimated prior proportions π_k 's can be used unchanged in the classification rule calculations. Using the above modified decision rule, we classified the 374 GRBs. Table 7a lists the results. It is clear from the table that Groups 1 and 3 have the highest number of the 374 GRBs classified to them and Group 2 the lowest. Table 7b lists the means of the parameters of the classified GRBs having incomplete information. We also present in Figure 9 a split violinplot (Hintze & Nelson 1998) with the left side of the violin displaying the distribution of the parameters from the 1599 GRBs and the right side displaying the distribution of the 374 GRBs which are missing observations in any other parameter.

The violin plots for the two duration variables $\log_{10} T_{50}$ and $\log_{10} T_{90}$ are very similar. The densities of the three peak

Table 6. (a) Number of GRBs classified to each of the five groups and (b) group means of the nine parameters for the classified GRBs. Note that this mean is computed for a parameter only for those GRBs that did not have missing observations in that parameter for that group.

Group	1	2	3	4	5
Number of observations	138	24	127	52	33

(a) Number of observations in each group

k	$\log T_{50}$	$\log T_{90}$	$\log F_1$	$\log F_2$	$\log F_3$	$\log F_4$	$\log P_{64}$	$\log P_{256}$	$\log P_{1024}$
1	0.72	1.12	-6.80	-6.49	-5.94	-0.16	-0.30	-0.16	-0.30
2	0.97	1.56	-6.32	-6.18	-5.91	-3.95	0.36	0.31	0.17
3	1.26	1.70	-6.33	-6.28	-6.02	-8.07	0.01	-0.06	-0.13
4	-0.45	0.39	-7.92	-7.95	-7.34	-6.62	0.19	-0.11	-0.61
5	-0.78	-0.38	-8.10	-7.84	-7.17	-0.18	0.17	-0.01	-0.44

(b) Mean parameter values for each group

fluxes $\log_{10} P_{64}$, $\log_{10} P_{256}$, $\log_{10} P_{1024}$ have heavier tails for the 1599 GRBs compared to that of the 374 GRBs with incomplete observations and are also more skewed for the 1599 GRBs. The 374 GRBs with missing parameter observations show a good degree of symmetry in all the three peak fluxes. It is also interesting to note that the 374 GRBs having incomplete observations in the four time integrated fluences have a much higher peak flux compared to the 1599 GRBs having complete observations in all the parameters. The density of the four fluences $\log_{10} F_1$, $\log_{10} F_2$, $\log_{10} F_3$, $\log_{10} F_4$ are also fairly similar in both cases. Thus it is evident that the GRBs having incomplete observations in the parameters have the tendency to have higher peak fluxes compared to the 1599 GRBs. This finding points to the possibility that they have generated a much higher energy compared to the 1599 GRBs with complete information. Finally, we note that our classification strategy does not have the ability to find (potentially) additional classes in the GRBs with missing parameters because we are using the classes found from clustering the 1599 GRBs in the assignment. Therefore, it would be desirable to have methodology that groups GRBs with missing and complete observations in a holistic approach. Development of such a statistical approach, while necessary, is however beyond the scope of this paper.

4 CONCLUSIONS

Many authors have attempted to determine the optimal number of kinds of GRBs in the BATSE catalogue using various statistical techniques. While most authors have suggested that the optimal number of groups are two, a few others have claimed this number to be three and not two. Recently Chattopadhyay & Maitra (2017) classified 1599 GRBs using GMMBC using six variables (three original and three derived) and found the optimal number of groups to be five. They presented various careful evidences in support of their findings. Motivated by the fact that the nine original variables might contain useful clustering information we carried out MBC using the nine original variables after checking for redundancy amongst them. Clustering the 1599 GRBs using

t MMBC showed that the optimal number of homogeneous groups is five which further supports of the results obtained by Chattopadhyay & Maitra (2017) and provides evidence that the additional ellipsoidal groups found by them can not be subsumed inside groups with heavier tails. These groups are also more distinct than the groups obtained in Chattopadhyay & Maitra (2017) as per the overlap measure of Maitra & Melnykov (2010). The bursts in Group 4 are long duration high fluence bursts while those in Group 1 are long duration fluence bursts. Bursts in Group 5 can thus be designated as high duration bursts with an intermediate fluence. Bursts in Groups 2 and 3 are short duration bursts and also have the lowest fluences. We also classified the 374 GRBs in the BATSE catalogue having incomplete observations in some of the parameters using a Bayes classifier to the five t MMBC groups obtained from clustering the 1599 GRBs. Comparison between the complete and partially observed GRBs was facilitated using a split violin plot for each of the nine observed parameters and indicates that the GRBs with missing observations in some of the parameters are likely to be high energy GRBs. This finding arises from the split violin plot where the densities of the peak fluxes are seen to be higher in GRBs with missing observations for some parameters as compared to those GRBs with observations in all parameters.

There are a number of issues which can be looked upon as a potential research problem. For one, it would be useful to incorporate and further develop clustering methods that have the ability to group observations that are complete and missing information in a holistic manner. Methodology and software would be helpful to develop in this scenario. Further, use of the logarithmic transformation, while standard in GRB classification, may obfuscate further group structure so that an approach which incorporates finding the transformation within the context of clustering would be worthwhile to explore. Finally, the analysis in this paper can be extended to GRBs catalogued from sources such as the datasets from the *Swift* and *Fermi* satellites to analyze whether similar results hold for GRBs observed from other satellites or not.

ACKNOWLEDGMENTS

We sincerely thank Professors Asis Kumar Chattopadhyay and Tanuka Chattopadhyay for originally introducing us to this research problem.

References

- Abramowitz M., Stegun I. A., 1964, Handbook of Mathematical Functions with Formulas, Graphs, and Mathematical Tables, Ninth Dover printing, tenth GPO printing edn. Dover, New York
- Andrews J. L., McNicholas P. D., 2012, Statistics and Computing, 22, 1021
- Andrews J. L., McNicholas P. D., 2015, teigen: Model-based clustering and classification with the multivariate t-distribution
- Bernardo J. M., Smith A. F. M., 1993, Bayesian Theory. Wiley
- Chattopadhyay S., Maitra R., 2017, Monthly Notices of the Royal Astronomical Society, 469, 3374
- Chattopadhyay T., Misra R., Chattopadhyay A. K., Naskar M., 2007, ApJ, 667, 1017
- Chen W.-C., Maitra R., 2011, Statistical Analysis and Data Mining, 4, 567
- Dempster A. P., Laird N. M., Rubin D. B., 1977, Journal of the Royal Statistical Society, Series B, 39, 1
- Dezalay J.-P., Barat C., Talon R., Syunyaev R., Terekhov O., Kuznetsov A., 1992, in Paciesas W. S., Fishman G. J., eds, American Institute of Physics Conference Series Vol. 265, American Institute of Physics Conference Series. pp 304–309
- Fraley C., Raftery A. E., 1998, The Computer Journal, 41, 578
- Fraley C., Raftery A. E., 2002a, Journal of the American Statistical Association, 97, 611
- Fraley C., Raftery A. E., 2002b, Journal of the American Statistical Association, 97, 611
- Fraley C., Raftery A. E., Murphy T. B., Scrucca L., 2012, mclust Version 4 for R: Normal Mixture Modeling for Model-Based Clustering, Classification, and Density Estimation
- Hintze J. L., Nelson R. D., 1998, The American Statistician, 52, 181
- Horváth I., 1998, ApJ, 508, 757
- Horváth I., 2002, A&A, 392, 791
- Horváth I., 2009, Ap&SS, 323
- Horváth I., Tóth B. G., 2016, Ap&SS, 361, 155
- Horváth I., Balázs L. G., Bagoly Z., Veres P., 2008, A&A, 489, L1
- Hubert L., Arabie P., 1985, Journal of Classification, 2, 193
- Huja, D. Mészáros, A. Rípa, J. 2009, A&A, 504, 67
- Inselberg A., 1985, The Visual Computer, 1, 69
- Johnson R. A., Wichern D. W., eds, 1988, Applied Multivariate Statistical Analysis. Prentice-Hall, Inc., Upper Saddle River, NJ, USA
- Kass R. E., Raftery A. E., 1995, Journal of the American Statistical Association, 90, 773
- Kouveliotou C., Meegan C. A., Fishman G. J., Bhat N. P., Briggs M. S., Koshut T. M., Paciesas W. S., Pendleton G. N., 1993, ApJ, 413, L101
- Kulkarni S., Desai S., 2017, Ap&SS, 362, 70
- Maitra R., 2001, Technometrics, 43, 336
- Maitra R., 2009, IEEE/ACM Transactions on Computational Biology and Bioinformatics, 6, 144
- Maitra R., 2010, NeuroImage, 50, 124
- Maitra R., Melnykov V., 2010, Journal of Computational and Graphical Statistics, 19, 354
- Maitra R., Melnykov V., Lahiri S., 2012, Journal of the American Statistical Association, 107, 378
- Mazets E. P., et al., 1981, Ap&SS, 80, 3
- McLachlan G., Krishnan T., 2008, The EM Algorithm and Extensions, second edn. Wiley, New York, doi:10.2307/2534032
- McLachlan G. J., Peel D., 1998, in Amin A., Dori D., Pudil P., Freeman H., eds, Advances in Pattern Recognition: Joint IAPR International Workshops SSPR'98 and SPR'98 Sydney, Australia, August 11–13, 1998 Proceedings. Springer Berlin Heidelberg, Berlin, Heidelberg, pp 658–666, doi:10.1007/BFb0033290
- McLachlan G., Peel D., 2000, Finite Mixture Models. John Wiley and Sons, Inc., New York, doi:10.1002/0471721182
- Melnykov V., Maitra R., 2010, Statist. Surv., 4, 80
- Melnykov V., Maitra R., 2011, Journal of Machine Learning Research, 12, 69
- Melnykov V., Chen W.-C., Maitra R., 2012, Journal of Statistical Software, 51, 1
- Meng X.-L., Rubin D. B., 1993, Biometrika, 80, 267
- Meng X.-L., Van Dyk D., 1997, Journal of the Royal Statistical Society: Series B (Statistical Methodology), 59, 511
- Modak S., Chattopadhyay A. K., Chattopadhyay T., 2017, Communications in Statistics - Simulation and Computation, 0, 1
- Mukherjee S., Feigelson E. D., Jogesh Babu G., Murtagh F., Fraley C., Raftery A., 1998, ApJ, 508, 314
- Nakar E., 2007, Physics Reports, 442, 166
- Norris J. P., Cline T. L., Desai U. D., Teegarden B. J., 1984, Nature, 308, 434
- Paczynski B., 1998, ApJ, 494, L45
- Pendleton G. N., et al., 1997, The Astrophysical Journal, 489, 175
- R Core Team 2017, R: A Language and Environment for Statistical Computing. R Foundation for Statistical Computing, Vienna, Austria, <https://www.R-project.org/>
- Raftery A. E., Dean N., 2006, Journal of the American Statistical Association, 101, 168
- Rand W. M., 1971, Journal of the American Statistical Association, 66, 846
- Schwarz G., 1978, Ann. Statist., 6, 461
- Tarnopolski M., 2015, A&A, 581, A29
- Wegman E., 1990, Journal of the American Statistical Association, 85, 664
- Woosley S., Bloom J., 2006, ARA&A, 44, 507
- Zhang Z.-B., Yang E.-B., Choi C.-S., Chang H.-Y., 2016, MNRAS, 462, 3243
- Zitouni H., Guessoum N., Azzam W. J., Mochkovitch R., 2015, Ap&SS, 357, 7
- Rípa J., Mészáros A., Wigger C., Huja D., Hudec R., Hajdas W., 2009, A&A, 498, 399

This paper has been typeset from a \TeX / \LaTeX file prepared by the author.